## Dissecting genetic risk in common and rare inherited disorders

Lahrouchi, N.

**Publication date**
2020
**Document Version**
Other version
**License**
Other

# CHAPTER 8

## Bi-allelic loss-of-function variants in *PLD1* cause congenital right-sided cardiac valve defects and neonatal cardiomyopathy

Najim Lahrouchi*, Alex V. Postma*, Christian M. Salazar, Daniel M. De Laughter, Fleur Tjong, Lenka Piherová, Forrest Z. Bowling, Dominic Zimmerman, Elisabeth M. Lodder, Asaf Ta-Shma, Zeev Perles, Leander Beekman, Aho Ilgun, Quinn Gunst, Mariam Hababa, Doris Škorić-Milosavljević, Viktor Stránecký, Viktor Tomek, Peter de Knijff, Rick de Leeuw, Jamille Y. Robinson, Sabrina C. Burn, Hiba Mustafa, Matthew Ambrose, Timothy Moss, Jennifer Jacober, Dmitriy M. Niyazov, Andreas Rousounides, Aphrodite Aristidou-Kallika, George Tanteles, Bruel Ange-Line, Anne-Sophie Denommé-Pichon, Christine Francannet, Damara Ortiz, Monique C. Haak, Arend D. J. Ten Harkel, Gwendolyn T.R. Manten, Annemiek C. Dutman, Katelijne Bouman, Monia Magliozzi, Francesca Clementina Radio, Gijs W.E. Santen, Johanna C. Herkert, Orly Elpeleg, Maurice J.B. van den Hoff, Barbara Mulder, Michael V. Airola, Stanislav Kmoch, Joey V. Barnett, Sally-Ann Clur, Michael A. Frohman and Connie R. Bezzina

* These authors contributed equally

**SUBMITTED**

## ABSTRACT

Congenital heart disease is the most common type of birth defect, accounting for one-third of all congenital anomalies. Using whole-exome sequencing in 2,718 congenital heart disease cases and a search in GeneMatcher, we identified 29 patients from 20 unrelated families of different ancestries with bi-allelic *PLD1* variants that presented predominantly with congenital cardiac valve defects. We also associate recessive *PLD1* variants with isolated neonatal cardiomyopathy. Furthermore, we established that p.I668F is a founder variant among Ashkenazi Jews (allele frequency ~2%) and describe the phenotypic spectrum of *PLD1*-associated congenital heart defects. PLD1 missense variants are over-represented in regions of the protein critical for catalytic activity and, correspondingly, a strong reduction in enzymatic activity was observed for most of the mutant proteins in an enzymatic assay. Finally, we demonstrate that PLD1 inhibition decreases epithelial-mesenchymal transformation, an established pivotal early step in valvulogenesis. In conclusion, this study provides an increased understanding of disease mechanisms and phenotypic expression associated with PLD1 loss-of-function.

# INTRODUCTION

Congenital heart disease is the most common type of birth defect, accounting for one-third of all congenital anomalies, with a worldwide occurrence of 7 per 1000 live births.[1] Right-sided congenital heart disease includes abnormalities of the pulmonary and tricuspid valves, the right ventricle and the right ventricular outflow tract. The genetic underpinnings of this group of disorders remain largely unexplored. Recessive variants in *PLD1*, which encodes phospholipase D1, a signal transduction enzyme that hydrolyses the membrane lipid phosphatidylcholine to generate the lipid second messenger phosphatidic acid, were recently associated with severe congenital cardiac valve defects in two small families.[2] While no overt structural cardiac defects were noted, mice lacking PLD1 display moderately impaired function of the pulmonary and tricuspid valve on echocardiography.[2] However, the functional consequences on PLD1 enzymatic activity and the mechanism by which PLD1 dysfunction leads to congenital valve abnormalities remain unknown.

Using whole-exome sequencing data from 2,718 congenital heart disease cases and a search in GeneMatcher[3], we identified 29 patients from 20 unrelated families of different ancestries with bi-allelic *PLD1* variants. We established that p.I668F is a founder variant among Ashkenazi Jews. We expanded the phenotypic spectrum of *PLD1*-associated congenital heart defects and for the first time provided evidence that recessive variants in *PLD1* can also cause neonatal cardiomyopathy in the absence of congenital heart defects. Placement of the missense variants on the three-dimensional crystal structure of PLD1, recently reported by some of the co-authors[4], localized them primarily to sites important for catalytic site integrity. Correspondingly, by functional analysis we uncovered a substantial loss of enzymatic activity. Finally, in line with a loss-of-function mechanism of PLD1, we demonstrated that PLD1 inhibition decreases epithelial-mesenchymal transformation (EMT), a pivotal early step in valvulogenesis.[5]



# METHODS

## Case recruitment and DNA sequencing

The index patient in Family A was enrolled at the Amsterdam UMC in Amsterdam, The Netherlands. Family B was identified among 75 unrelated patients with severe right-sided valvular congenital heart disease (i.e. Tricuspid atresia or stenosis, Ebstein's anomaly or pulmonary atresia) from the National Registry and DNA bank of congenital heart defects (CONCOR)[6] in The Netherlands. We subsequently used GeneMatcher[3] and analysis of 2,643 congenital heart disease trios (i.e. the affected case and both parents) who underwent

whole-exome sequencing from the Pediatric Cardiac Genomics Consortium (PCGC)[7,8], to identify other patients with bi-allelic variants in *PLD1*. Details on case recruitment and next-generation sequencing methods for each family can be found in the **Supplemental Data**.

### cDNA analysis of c.3000+2T>A *PLD1* splicing variant and proband carrying p.G826R/p.G910V

Total RNA was isolated from peripheral mononuclear blood cells using TRIzol solution (ThermoFischer Scientific). RNA concentrations were determined spectrophotometrically at A260 nm by NanoDrop (NanoDrop Technologies, Wilmington, DE), and RNA quality was verified using an Agilent 2100 bioanalyser - RNA Lab-On-a-Chip (Agilent Technologies, Santa Clara, USA). Aliquots of isolated RNA were stored at -80°C until analysis. The first-strand cDNA synthesis was carried out using an oligo-dT primer and either SuperScript® III Reverse Transcriptase (ThermoFisher Scientific). PLD1 cDNA was PCR-amplified from the synthesized first-strand cDNA using oligonucleotide primers (Generi Biotech, Hradec Králové, Czech Republic) designed to span and amplify the variant-bearing PLD1 sequence. The resultant PCR products were analyzed using agarose gel electrophoresis. Individual DNA fragments were extracted from gel slices using PureLink Quick Gel Extraction Kit (ThermoFisher Scientific) and sequenced by direct Sanger sequencing as described above. Regarding the p.G826R/p.G910V cDNA, it was subcloned into pcDNA3.1 (Invitrogen), and Sanger sequenced to determine if the variants were on the same strand.

### Plasmid constructs, cell line and transfections

We purchased a human *PLD1* cDNA clone (BC068976) set in a pGEM-T plasmid (Sino Biological Inc.). The clone was fully sequence verified and contained no nucleotide changes. Variants were introduced using site-directed mutagenesis (Q5, NEB) and the mutant constructs were fully verified by sequencing. Next the wildtype and mutant cDNA clones were subcloned into a pcDNA3.1(+) vector for expression and sequence verified. The COS7 cells were cultured according to standard methods. Transfections were performed using polyethylenimine (PEI) in a plasmid to PEI ratio of 1:4.

### *In Vivo* PLD Activity

Enzymatic activity was measured based on PLD1's ability to catalyze a transphosphatidylation reaction using 1-butanol to generate phosphatidylbutanol.[9] HEK293T cells were incubated overnight in a 6-well plate and transfected in full media the next day with PLD1 expression plasmids using Fugene (Promega). 12-16 hours post overnight transfection, the cells were labelled with [$^3$H]-palmitate (ART 129; American Radiolabeled Chemicals) and cultured for 24 hours. The radiolabeled media was then

replaced with Opti-MEM and the cells cultured for 1-2 hours prior to the addition of 0.3% butanol and 100nM PMA. After 30 minutes, cold methanol was added to stop the reaction and the lipids extracted and dried using a speed vacuum, and resuspended in chloroform/methanol (19:1) containing 50 mg of non-radiolabeled phosphatidylbutanol (Avanti Polar Lipids) to enable location of the labelled enzymatic product on TLC plates (Whatman LK5DF). The plates were then developed as previously described[9] and the lipids visualized using iodine flakes (Sigma-Aldrich) and scraped into 5 mL of scintillation fluid for quantification. In these studies, we used PLD1-K898R as a baseline control. K898 is located in the second of two highly conserved HxKxxxxD ("HKD") motifs (**Figure 1b**)[10] that constitute key functional elements of the two halves of the assembled core catalytic site.[11–13] A representative experiment showing the production of phosphatidylbutanol (PtdBut) by the wild-type allele and the absence of its production by the fully-inactive K898R allele is shown in **Supplementary Figure 4**. A limited amount of PtdBut production is observed in the K898R sample, which derives from the small amounts of endogenous, wild-type PLD1 and PLD2 present in the cell line used for the transfections. The percentage activity of mutant proteins was determined in comparison to the overexpressed wild-type PLD1 activity after subtraction off of the baseline activity observed with the fully-inactive K898R mutant allele.



### Western blot analysis

HEK293T cells were transfected with 2.5 mg of mutant Hemagglutinin (HA)-tagged PLD1 or wild-type PLD1 per well in a 6-well plate using Fugene (Promega). After 24-48 hours, the cells were collected in 60 mL of homogenization buffer (1mM DTT, 1mM EDTA, and 0.1mM PMSF in PBS) per well and sonicated using a micro tip sonicator at the lowest setting. 10 mL of lysate plus 10 mL of SDS-PAGE loading buffer containing 8M urea were combined and loaded onto an acrylamide gel for electrophoresis and transfer to nylon membrane. The PLD1 protein generated from the transfected expression vector was detected using a monoclonal anti-HA antibody (3F10; Sigma) followed by a secondary goat anti-rat antisera coupled to an infrared dye (IR800, Thermo). Images were recorded and bands quantitated using an Odyssey CLx system.

### *In vitro* collagen gel assay

Collagen gel assays (see ref[14]) with siRNA or small molecule additions were performed as described previously.[15] siRNA knockdown experiments have been described elsewhere.[16] Briefly, atrioventricular cushions (AVCs) were excised from stage 16 chick embryo hearts and were collected in M199 medium (Mediatech, Inc.) at room temperature for each experimental condition. For transfection, first 4 µl of siPORT NeoFX (Ambion) was incubated in a final volume of 100µl of M199 for 10 min at room temperature. Next, the appropriate

final concentration (for 300 µl of total volume) of siRNA was added to a final volume of 100 µl. These two tubes were mixed and incubated for 15 min at room temperature to allow complexes to form. Next, the 200-µl mixture was added to the 100 µl containing AVCs and this solution was incubated at 37 °C, 5% CO2 for 45 min. Explants were then placed endothelial side down on collagen gels (1.86mg/ml) and incubated under the same conditions for 48 h prior to fixation (0.8% formaldehyde, 0.05% glutaraldehyde for 5 min at room temperature). Control for siRNA toxicity were randomized GC matched constructs that do not correspond to any sequence in the chick genome. The following antisense strand siRNAs were used: PLD1-A, antisense strand siRNA: AUGGUGUACACGUUGAGGCtt, and PLD1-B: antisense strand siRNA: CUUAGCGUUCACAUACCACtt. The positive control was siRNA targeting *Tgfbr3*.[17] For experiments using small molecule inhibitors, AVCs were harvested and placed endothelial side down on collagen gels in the presence of the concentrations of molecules indicated. Explants were incubated for 48 h prior to fixation as above. After incubation, epithelial to mesenchymal transformation (EMT) was quantified by counting the number cells with mesenchymal morphology that invaded into the collagen gel.

## Principal component analysis to define ancestry of PCGC-CHD cases

Principal components analyses were performed in PLINK 2.0[18] on the WES PCGC cases, as previously described[19], using the 1000 Genomes populations (Phase3v5) and the ASJ individuals from the Gene Expression Omnibus database[20] (accession GSE23636) as a reference. To increase genetic overlap with the WES PCGC cases and the 1000 Genomes populations, we performed genome-wide imputation using Eagle2 phasing, Minimac3 and the Haplotype reference consortium (HRCr1.1) panel implemented on the Michigan Imputation Server for the ASJ dataset. After imputation we performed stringent genetic QC using hard genotype calls after imputation (genotype probability >0.9) and restricted to variants with an imputation score >0.8. We excluded variants with genotype missingness >0.01, Hardy-Weinberg equilibrium test P<0.05, phenotype-biased missing test P<0.05, and minor allele frequency (MAF) <0.05. Downstream analyses were conducted in R version 3.4.3.

## Haplotype analysis and variant dating

Haplotypes were generated using WES data. Estimation of the p.I668P variant age was conducted using the Gamma method.[21] This method uses the genetic length of ancestral haplotypes shared between individuals carrying the variant and has as a major advantage that it can be reliably applied to small samples with high-density SNP data.

# RESULTS AND DISCUSSION

## *PLD1* variants cause congenital valvular defects or neonatal cardiomyopathy in multiple families

To uncover the genetic cause of severe right-sided congenital heart defects in a consanguineous Afghan family with two affected siblings (Family A, **Figure 1a**), we performed whole-exome sequencing in both parents and one of the affected siblings. In line with the expected recessive inheritance pattern, we identified a homozygous variant p.R695C in *PLD1* (GenBank accession number: NM_002662) as the only co-segregating variant. We then searched for additional patients carrying bi-allelic variants in *PLD1* by performing (I) whole-exome sequencing in 75 patients with a similar severe right-sided congenital heart defects from the National Registry of congenital heart defects (CONCOR) in The Netherlands[6], (II) analysis of 2,643 congenital heart disease trios (i.e. the affected case and both parents) who underwent whole-exome sequencing from the Pediatric Cardiac Genomics Consortium (PCGC)[7,8], and (III) a search using GeneMatcher.[3] In total, we identified 29 patients from 20 unrelated families of different ancestries (**Figure 1a**, **Table 1**, **Supplemental Table 1**) carrying either homozygous or compound heterozygous *PLD1* variants. All 29 patients were diagnosed with severe congenital cardiac disease at the fetal or neonatal stage.



Twenty-seven patients from 18 families (Families A-R, **Figure 1**) presented with congenital cardiac valve malformations predominantly affecting the right side of the heart. These defects were characterized by severe tricuspid and/or pulmonary valve abnormalities (26/27), hypoplastic right ventricles (15/27), and/or hypoplastic pulmonary arteries (10/27) (**Table 1**, **Supplemental Table 1,** detailed phenotypic descriptions in **Supplemental Note 1,** echocardiography in a selection of patients in **Videos 1a-d**). Four out of these 27 patients were diagnosed with Ebstein's anomaly. The extremely thin right ventricular wall in both patients from Family A prompted a diagnosis of Uhl's anomaly, a rare heart defect characterized by congenital partial or complete absence of right ventricular wall myocardium (**Figure 1c**).[22] Two patients had dilated left ventricles and mitral regurgitation in addition to tricuspid and/or pulmonary valve defects. Six pregnancies were terminated because of a complex heart defect with poor prognosis (gestational age range 13-22 weeks). Four patients survived less than a year as a result of their underlying structural heart defect. The majority of live-born infants required surgery in the first days or months of life, most commonly the placement of a Blalock–Taussig shunt and bidirectional Glenn palliation (**Table 1**).

Of note, two patients presented with severe isolated neonatal cardiomyopathy (i.e. in the absence of a structural congenital heart defect), a new finding for this syndrome (Families S and T, **Figure 1**, **Table 1**). The patient from Family S presented at 33 weeks of gestation with persistently reduced fetal movement. Fetal ultrasound revealed hydrops fetalis due to severe cardiomyopathy and emergency delivery by caesarean section was performed. Postnatal echocardiography showed severe systolic dysfunction of the left ventricle with severe mitral regurgitation (**Supplemental Videos 1e and f**). Despite medical treatment, the child died on the third postnatal day due to intractable cardiac failure. The other patient (Family T) was a full-term neonate who developed difficulty breathing and bloody vomiting and died on postnatal day 8. The autopsy showed sections of the heart with patchy replacement of the myocardium by histiocytoid cells and occasional plasma cells and eosinophils, a finding most consistent with histiocytoid cardiomyopathy. Both patients were screened for variants in ~300 cardiomyopathy-related genes and were found negative.

Overall, none of the patients that survived beyond infancy had dysmorphic features, intellectual disability or notable developmental delay, suggesting that in the context of overt phenotypes, *PLD1* loss-of-function (see below) is predominantly associated with isolated cardiac disease.

An autosomal recessive mode of inheritance was observed in all of the families and variants in *PLD1* were inherited from each of the unaffected parents. In total, we report here 29 *PLD1* variants, of which 20 are missense variants and 9 are expected to result in protein truncation (**Supplemental Table 2**). Two variants are predicted to affect splicing. RT-PCR analysis of mRNA isolated from a peripheral blood sample from the parents of Family E confirmed mis-splicing that is predicted to result in a truncated PLD1 protein (**Supplemental Fig. 1**). The duplication of exons 13-21 found in Family F is predicted to result in a premature stop codon in exon 13. With two exceptions, the identified variants were not homozygous in 123,136 exomes and 15,496 genomes from the Genome Aggregation Database (gnomAD, accessed October 2019[23]), suggesting that homozygosity for these variants is not tolerated. The two exceptions are p.E6K and p.E290Q, which were found in compound heterozygosity with p.R712W in Family C and p.G237C in Family M, respectively. The gnomAD database contains 42 predicted loss-of-function *PLD1* variants (expected number, 62); none of them occur in the homozygous state, suggesting that *PLD1* is intolerant to homozygous loss-of-function variants. While eleven out of 29 variants were not present in gnomAD[23], the minor allele frequency (MAF) for the others ranged from 0.0008% to 0.16%.

**Table 1.** Clinical characteristics of patients with bi-allelic PLD1 variants

| Family | Patient | PLD1-variant (cDNA) | PLD1-variant (AA) | PLD1 enzymatic function (%) | Ethnicity | Sex | Status | Age | Tricuspid valve defect | Pulmonary valve defect | Hypoplastic right ventricle | Pulmonary artery hypoplasia | Mitral valve defect | Cardiomyopathy | Surgery/procedures (age) |
|---|---|---|---|---|---|---|---|---|---|---|---|---|---|---|---|
| Congenital heart defect | | | | | | | | | | | | | | | |
| Family A | II-1 | c.2083C>T/ c.2083C>T | p.R695C/ p.R695C | 5,7 | Afghan | F | deceased | 11mo | + | + | + | - | - | - | BTS (11mo) |
| | II-5 | | | | | F | TOP | 18wks | + | + | - | + | - | - | none (TOP) |
| Family B | II:1 | c.2729G>T/ c.2476G>A | p.G910V/ p.G826R | 2,8 | Dutch | F | alive | 40yrs | + | + | - | + | - | - | BTS, BGP, VSD and ASD closure, Fontan |
| Family C | II:1 | c.16G>A/ c.2134C>T | p.E6K/p.R712W | 75,0 | Bangladeshi | M | alive | 37wks | - | + | - | - | - | - | NA |
| Family D | II-1 | c.1085T>C/ c.1171C>T | p.F362S/ p.R391C | <67 | Cypriot | M | TOP | 15wks | + | + | + | + | - | - | none (TOP) |
| | II-2 | | | | | F | TOP | 16wks | + | + | + | + | - | - | none (TOP) |
| Family E | II-4 | c.1391A>G/ c.3000+2T>A | p.H464R/ p.V962FfsTer11 | 1,1 | Czech | M | TOP | 14wks | + | + | - | - | - | - | none (TOP) |
| | II-5 | | | | | M | TOP | 13wks | + | NA | - | NA | - | - | none (TOP) |
| Family F | II:1 | c.3142C>G/ duplication | p.P1048A/ duplication | 0,7 | Latino | M | alive | 11mo | - | - | - | - | - | - | - |
| | II:2 | | | | | M | alive | 11mo | - | + | - | - | - | - | balloon dilation PV (4mo) |
| | II:3 | | | | | M | alive | 11mo | + | + | + | - | - | LVNC | BGP, atrial septectomy and ligation of PDA (6mo) |
| Family G | II-1 | c.2002A>T/ c.2002A>T | p.I668F/p.I668F | 20,3 | Ashkenazi Jewish | M | alive | 5yrs | + | + | + | + | - | - | BTS and BGP awaiting Fontan TCPC procedure |
| | II-5 | | | | | F | deceased | 7d | + | + | + | + | - | - | none (deceased) |
| Family H | II-1 | c.2002A>T/ c.2002A>T | p.I668F/p.I668F | 20,3 | Ashkenazi Jewish | F | NA | NA | + | + | + | - | - | - | NA |
| Family I | II-1 | c.2002A>T/ c.2002A>T | p.I668F/p.I668F | 20,3 | Ashkenazi Jewish | F | NA | NA | - | + | + | - | - | - | NA |
| Family J | II-1 | c.2002A>T/ c.2236C>T | p.I668F/p.R746C | <60 | European | M | NA | NA | + | + | - | - | - | | NA |
| Family K | II-1 | c.2452T>C/ c.2452T>C | p.Y818H/ p.Y818H | not tested | East-Asian | F | NA | NA | + | - | - | - | - | - | NA |

**Table 1.** Continued

| Family | Patient | PLD1-variant (cDNA) | PLD1-variant (AA) | PLD1 enzymatic function (%) | Ethnicity | Sex | Status | Age | Tricuspid valve defect | Pulmonary valve defect | Hypoplastic right ventricle | Pulmonary artery hypoplasia | Mitral valve defect | Cardiomyopathy | Surgery/procedures (age) |
|---|---|---|---|---|---|---|---|---|---|---|---|---|---|---|---|
| Family L | II-1 | c.2023C>T/ c.2098C>T | p.R675W/ p.R700C | <50 | East-Asian | F | NA | NA | + | + | + | + | - | - | NA |
| Family M | II-1 | c.709G>T/c. G868G>C | p.G237C/ p.E290Q | 78 | European | M | NA | NA | - | - | - | - | + | - | NA |
| Family N * | II-1 | c.1325A>C/ c.1325A>C | p.H442P/ p.H442P | 7,1 | Middle-Eastern | F | deceased | 12mo | - | + | - | - | - | - | - |
| | II-3 | | | | | M | alive | 25yrs | + | + | + | - | - | - | CS (3yrs), BGP (5yrs), VSD closure, 1.5 ventricle repair (22yrs) |
| | II-4 | | | | | M | alive | 20yrs | + | + | + | + | - | | BTS (2wks), BGP (1yr), Fontan (16yrs) |
| Family O* | II-1 | c.1482_1483del/ c.2882+2T>C | p.T495RfsTer32/ c.2882+2T>C | 0 | Middle-Eastern | F | alive | 5yrs | + | - | - | - | + | - | MV repair (8mo) |
| | II-3 | | | | | M | alive | 20yrs | + | - | - | - | - | - | - |
| | II-4 | | | | | F | deceased | 21d | + | + | + | + | - | - | CS (5d) |
| Family P | II-1 | c.2098C>T/c. A2681A>C | p.R700C/ p.Y894S | not tested | Mixed Caucasian | M | deceased | 23d | + | + | + | - | - | - | - |
| Family Q | II-1 | c.1062G>A/ c.2681A>C | p.W354Ter/ p.Y894S | <50% | French | F | fetal death | 16wks | + | + | + | - | - | - | - |
| Family R | II-3 | c.892C>T/ c.2415delC | p.R298Ter/ p.L806fsTer0 | 0 | Dutch | F | TOP | 19wks | + | + | + | + | - | - | none (TOP) |
| Neonatal cardiomyopathy | | | | | | | | | | | | | | | |
| Family S | II:2 | c.2542A>T/ c.2191A>T | p.R848Ter/ p.R731Ter | 0 | Dutch | M | deceased | 3d | - | - | - | - | - | DCM | - |
| Family T | II:2 | c.1403T>A/ c.2024G>A | p.V468D/ p.R675Q | 2,5 | Latino | M | deceased | 8d | - | - | - | - | - | Histiocytoid CMP | - |

**Abbreviations:** *Age: d, days; wks, weeks; mo, months; yrs, years, ASD: atrial septal defect, BTS: Blalock-Taussig shunt, BGP: bidirectional Glenn procedure, CMP: cardiomyopathy, CS: central shunt, DCM: dilated cardiomyopathy, LVNC: left ventricular non-compaction cardiomyopathy, MV: mitral valve, NA: not available, PDA: persistent ductus arteriosus, TOP: termination of pregnancy, Sex: F for Female and M for Male, TCPC: Total Cavopulmonary Connection, VSD: ventricular septal defect. *previously published family[2] Families H-M were identified through analysis of Pediatric Cardiac Genomics Consortium (PCGC) data.[7,8] + phenotype present, – phenotype absent. Variants were annotated on transcript: NM_002662. For a more detailed phenotype description see* **Supplementary Table 1**.

## The p.I668F missense variant in *PLD1* is a founder variant among Ashkenazi Jews

Given that in three families the same homozygous *PLD1* variant p.I668F was found, we hypothesized whether this is a founder variant. Intriguingly, all three homozygous *PLD1* p.I668F congenital heart defect families were of Ashkenazi Jewish ancestry, suggesting a novel founder variant. Ashkenazi Jewish descent was self-reported for Family G and determined through principal component analysis for Families H and I, which were recruited through PCGC and found to cluster with an Ashkenazi Jewish reference population[20] (**Supplemental Fig. 2**). As expected for a founder variant, all homozygous patients shared p.I668F on the background of a common haplotype spanning ~881-kb (chr3:171087469-171969077, hg19). Using the Gamma method[21], we estimated the age of the p.I668F founder variant at 46 generations (95% confidence interval (CI) 15-154 generations). Assuming a 20-year generation span, a common ancestor with this haplotype would have lived ~920 years ago (CI 300-3080 years). Interestingly, p.I668F has a MAF of ~2% among the Ashkenazi Jewish subpopulation in gnomAD and is rare among the other populations (0.004%-0.14%).[23] This finding has clinical implications for assessing risk of congenital heart defects among Ashkenazi Jews, since up to ~1 out 2500 births among Ashkenazi Jews would be homozygous for p.I668F.[23] As comparison, a recessive founder variant in *GDF1* (MAF in Ashkenazi Jewish subpopulation in gnomAD ~0.9%) was recently found to account for approximately 5% of severe congenital heart defects in Ashkenazi Jews.[8]

## Reduced PLD1 enzymatic activity associates with cardiac valvular defects or neonatal cardiomyopathy

Placement of the 20 missense variants described above onto the PLD1 structure revealed that they largely cluster in the highly conserved HxKxxxxD ("HKD") domains and the C-terminal region (**Figure 1b**) that are critical for enzymatic activity.[24] In contrast, 18 presumed non-deleterious *PLD1* variants found homozygously in the general population (as per gnomAD[23], MAF range: 0.001%-18%) distribute along the entire length of the protein, including in the N-terminus, PX and PH domains, and loop regions that are dispensable for catalytic activity.[24] Of note, while 5/18 variants that were found in the homozygous state in gnomAD resided in the loop region of PLD1, none of the patients carried a variant in the PLD1 loop region (**Figure 1b,** P=0.017).

To test their effect on PLD1 enzymatic activity, we engineered the disease-associated missense variants into an HA-tagged wild-type PLD1 expression vector[25] and transfected them into HEK293 cells. Western blot analysis showed levels of expression of the mutant proteins that were comparable to that seen for wild-type PLD1 and for PLD1-p.K898R, a

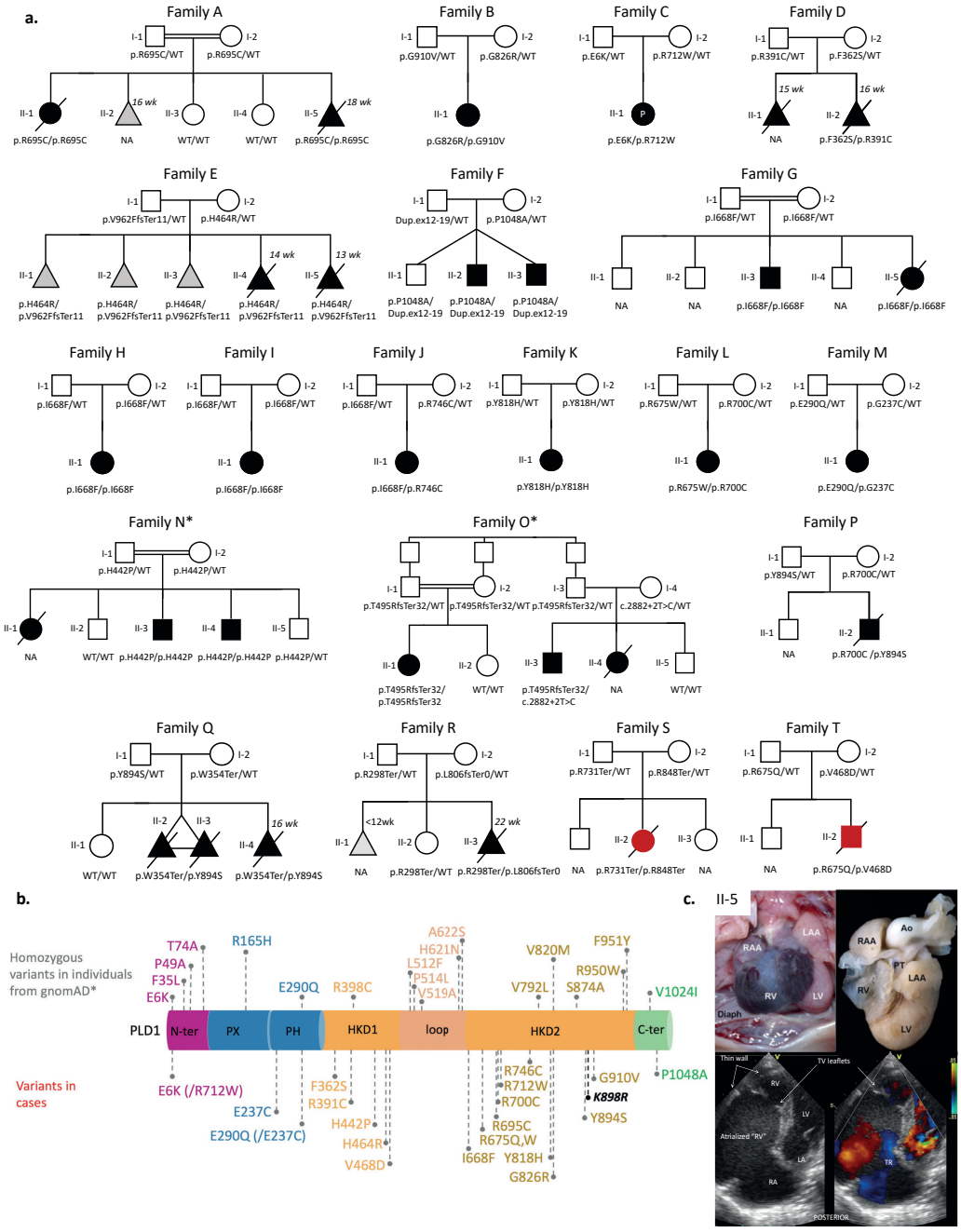
a.
Family A
I-1 p.R695C/WT
I-2 p.R695C/WT
II-1 p.R695C/p.R695C
II-2 16 wk NA
II-3 WT/WT
II-4 WT/WT
II-5 18 wk p.R695C/p.R695C
Family B
I-1 p.G910V/WT
I-2 p.G826R/WT
II-1 p.G826R/p.G910V
Family C
I-1 p.E6K/WT
I-2 p.R712W/WT
II-1 P p.E6K/p.R712W
Family D
I-1 p.R391C/WT
I-2 p.F362S/WT
II-1 15 wk NA
II-2 16 wk p.F362S/p.R391C
Family E
I-1 p.V962FfsTer11/WT
I-2 p.H464R/WT
II-1 p.H464R/p.V962FfsTer11
II-2 p.H464R/p.V962FfsTer11
II-3 p.H464R/p.V962FfsTer11
II-4 14 wk p.H464R/p.V962FfsTer11
II-5 13 wk p.H464R/p.V962FfsTer11
Family F
I-1 Dup.ex12-19/WT
I-2 p.P1048A/WT
II-1 p.P1048A/Dup.ex12-19
II-2 p.P1048A/Dup.ex12-19
II-3 p.P1048A/Dup.ex12-19
Family G
I-1 p.I668F/WT
I-2 p.I668F/WT
II-1 NA
II-2 NA
II-3 p.I668F/p.I668F
II-4 NA
II-5 p.I668F/p.I668F
Family H
I-1 p.I668F/WT
I-2 p.I668F/WT
II-1 p.I668F/p.I668F
Family I
I-1 p.I668F/WT
I-2 p.I668F/WT
II-1 p.I668F/p.I668F
Family J
I-1 p.I668F/WT
I-2 p.R746C/WT
II-1 p.I668F/p.R746C
Family K
I-1 p.Y818H/WT
I-2 p.Y818H/WT
II-1 p.Y818H/p.Y818H
Family L
I-1 p.R675W/WT
I-2 p.R700C/WT
II-1 p.R675W/p.R700C
Family M
I-1 p.E290Q/WT
I-2 p.G237C/WT
II-1 p.E290Q/p.G237C
Family N*
I-1 p.H442P/WT
I-2 p.H442P/WT
II-1 NA
II-2 WT/WT
II-3 p.H442P/p.H442P
II-4 p.H442P/p.H442P
II-5 p.H442P/WT
Family O*
I-1 p.T495RfsTer32/WT
I-2 p.T495RfsTer32/WT
I-3 p.T495RfsTer32/WT
I-4 c.2882+2T>C/WT
II-1 p.T495RfsTer32/p.T495RfsTer32
II-2 WT/WT
II-3 p.T495RfsTer32/c.2882+2T>C
II-4 NA
II-5 WT/WT
Family P
I-1 p.Y894S/WT
I-2 p.R700C/WT
II-1 NA
II-2 p.R700C /p.Y894S
Family Q
I-1 p.Y894S/WT
I-2 p.W354Ter/WT
II-1 WT/WT
II-2 p.W354Ter/p.Y894S
II-3
II-4 16 wk p.W354Ter/p.Y894S
Family R
I-1 p.R298Ter/WT
I-2 p.L806fsTer0/WT
II-1 <12wk NA
II-2 p.R298Ter/WT
II-3 22 wk p.R298Ter/p.L806fsTer0
Family S
I-1 p.R731Ter/WT
I-2 p.R848Ter/WT
II-1 NA
II-2 p.R731Ter/p.R848Ter
II-3 NA
Family T
I-1 p.R675Q/WT
I-2 p.V468D/WT
II-1 NA
II-2 p.R675Q/p.V468D
b.
Homozygous variants in individuals from gnomAD*
T74A
P49A
F35L
E6K
R165H
E290Q
R398C
A622S
H621N
L512F
P514L
V519A
V820M
V792L
F951Y
R950W
S874A
V1024I
PLD1
N-ter
PX
PH
HKD1
loop
HKD2
C-ter
Variants in cases
E6K (/R712W)
E237C
E290Q (/E237C)
F362S
R391C
H442P
H464R
V468D
I668F
R675Q,W
Y818H
G826R
R746C
R712W
R700C
R695C
K898R
Y894S
G910V
P1048A
c.
II-5
RAA
LAA
RV
LV
Diaph
Ao
PT
Thin wall
TV leaflets
Atrialized "RV"
LA
RA
TR
POSTERIOR

**Figure 1. Recessive variants in *PLD1* cause a spectrum of valvular congenital heart disease and neonatal cardiomyopathy** (**a**) Pedigrees; Filled-in symbols indicate affected individuals (black, congenital heart defect; red, fetal/neonatal cardiomyopathy) and symbols with a slash through them indicate deceased individuals. A double line indicates consanguinity. Males are indicated by squares and females by circles. Black filled-in triangle with a slash through them indicates fetal death or termination of pregnancy. Grey filled-in triangle indicates a miscarriage. Abbreviations: Dup, duplication; Ex, exon; Fs, frame-shift; WT, wild type; Ter, termination; wk, age in weeks at termination of pregnancy. *previously published family[2] Families H-M were identified through analysis of Pediatric Cardiac Genomics Consortium (PCGC) data and pedigrees were not available.[7,8] (**b**) PLD1 domain structure and location of pathologic (bottom) and presumptive non-pathologic (top) missense variants. ***Black***, inactive allele[13] used as baseline control. *homozygous missense variants found in gnomAD individuals.[23] (**c**) Macroscopic appearance of the heart of fetus II-5 from Family A. **Left upper panel:** position of the heart in the thorax. Note the extremely dilated RV with a thin translucent wall. A sharp demarcation can be seen between the abnormal right ventricular myocardium and normal left ventricular myocardium. **Right upper panel:** anterior view of formalin-fixed cardiac specimen including large vessels showing the paper-thin right ventricular wall, partially collapsed due to the tissue-weakness. **Bottom panels:** postnatal echocardiography of child II-1 from Family A displaying a thin walled right ventricle with Ebstein's anomaly of the tricuspid valve and tricuspid regurgitation (**Supplemental Video 1**). This child also had pulmonary atresia. **Abbreviations:** Ao, ascending aorta; Diaph, thoracic diaphragm; LA, left atrium; LAA, left atrial appendage; LV, left ventricle; PT, pulmonary trunk; RAA, right atrial appendage; RV, right ventricle; TV, tricuspid valve; TR, tricuspid regurgitation.

previously shown catalytically-inactive variant (**Supplemental Fig. 3**).[13] Enzymatic activity was assessed using an *in vivo* transphosphatidylation assay in the presence of phorbol myristate acetate (PMA), which activates protein kinase C (PKC), a potent stimulator of PLD1 activity.[10,13] PLD1-p.K898R[13] was used as a baseline control (**Supplemental Figure 4**). We observed a strong to dramatic reduction in PLD1 enzymatic activity for 13 of the 15 variants tested, leading to the prediction that patients carrying bi-allelic *PLD1* variants will generally have <25% residual PLD1 activity in comparison to individuals with wild-type *PLD1* alleles (**Fig. 2a)**. Of note, the two variants that occurred in the homozygous state in individuals from gnomAD (i.e. p.E6K and p.E290Q) and compound heterozygously in the patients did not affect PLD1 enzymatic activity.

Since an intact C-terminus is required for enzymatic activity[4,24], we expect that all of the variants resulting in premature termination of PLD1 protein, such as p.R731Ter/p.R848Ter in the isolated-cardiomyopathy patient from Family S, would fully eliminate PLD1 activity. Of note, the other patient presenting with isolated cardiomyopathy (Family T) was compound heterozygous for two missense variants (p.V468D/p.R675Q) that result in drastically reduced catalytic activity (2.5% compared to WT). Thus, residual PLD1 enzymatic activity of variants from patients presenting with isolated cardiomyopathy was similar to that of patients who presented with structural cardiac malformations. Taken together, these data suggest that unknown factors may modulate the phenotypic outcome of variants that reduce or ablate PLD1 function.

## PLD1 disease-associated variants localize to sites important for catalytic activity

Some of us recently reported the crystal structure for a catalytically-functional PLD1 protein (representing ~60% of the protein)[4] that encompasses most of the disease-associated variants reported in this study. **Figure 2b** shows the placement of 17 of the 20 disease-associated missense variants reported here on the 3-dimensional structure (see also **Supplemental Videos 2-18**). Placement of the remaining three variants was not assessed as these were located in the N-terminal (p.E6K) and PH-domain region (p.E237C and p.E290Q) of the PLD1 protein and were not included in the crystal structure.[4] Strikingly, the majority of the missense variants cluster near sites critical for catalytic activity, which is consistent with their resulting in a reduction of PLD1 enzyme activity.

We categorized these variants into three groups according to their predicted disruptive affects (**Figure 2b**). (1) The first class of variants affect the active site of PLD1. These variants either alter a residue directly involved in catalysis (p.H464) or are located within the active site (p.G826, p.Y894 and p.G910), thus affecting catalysis. (2) The second class of variants stabilize elements that form the binding site for the membrane lipid phosphatidylinositol-4,5-bisphosphate ($PI(4,5)P_2$), which is a required co-factor for PLD1 activity.[4,25] These residues include p.R695, which was mutated in the index family (Family A) of our study, as well as p.H442, p.R712, and p.R746. Mutation of these residues are predicted to alter the $PI(4,5)P_2$ binding site and decrease PLD1 activity. (3) The majority and remaining variants fall into a third class, which are distributed throughout the catalytic domain. The mutated residues are buried within the correctly folded structure and are involved in interactions with neighbouring residues. These variants would destabilize local interaction networks presumably necessary for proper folding or create new unfavourable interactions. A notable example is the p.I668F founder variant in Ashkenazi Jews. For this variant, substitution with the larger phenylalanine sidechain is predicted to create steric clashes with nearby residues that form part of the substrate-binding pocket (**Supplemental Video 7**). These clashes would alter the shape of the pocket, thus diminishing PLD1 activity.

Only three of the variants that we identified in the patients were found outside the catalytic domain. These were located at either the extreme N-terminus (p.E6K) or within the PH domain (p.G237C and p.E290Q), which is required for proper localization of PLD1 to the plasma membrane. As discussed above, both p.E6K (Family C) and p.E290Q (Family M) seem to be tolerated in the homozygous state and were associated with disease only in combination with p.R712W or p.G237C, respectively. Furthermore, these two variants retained full PMA-stimulated enzyme activity. Their exact role in determining the congenital heart defect phenotype in combination with the mutant

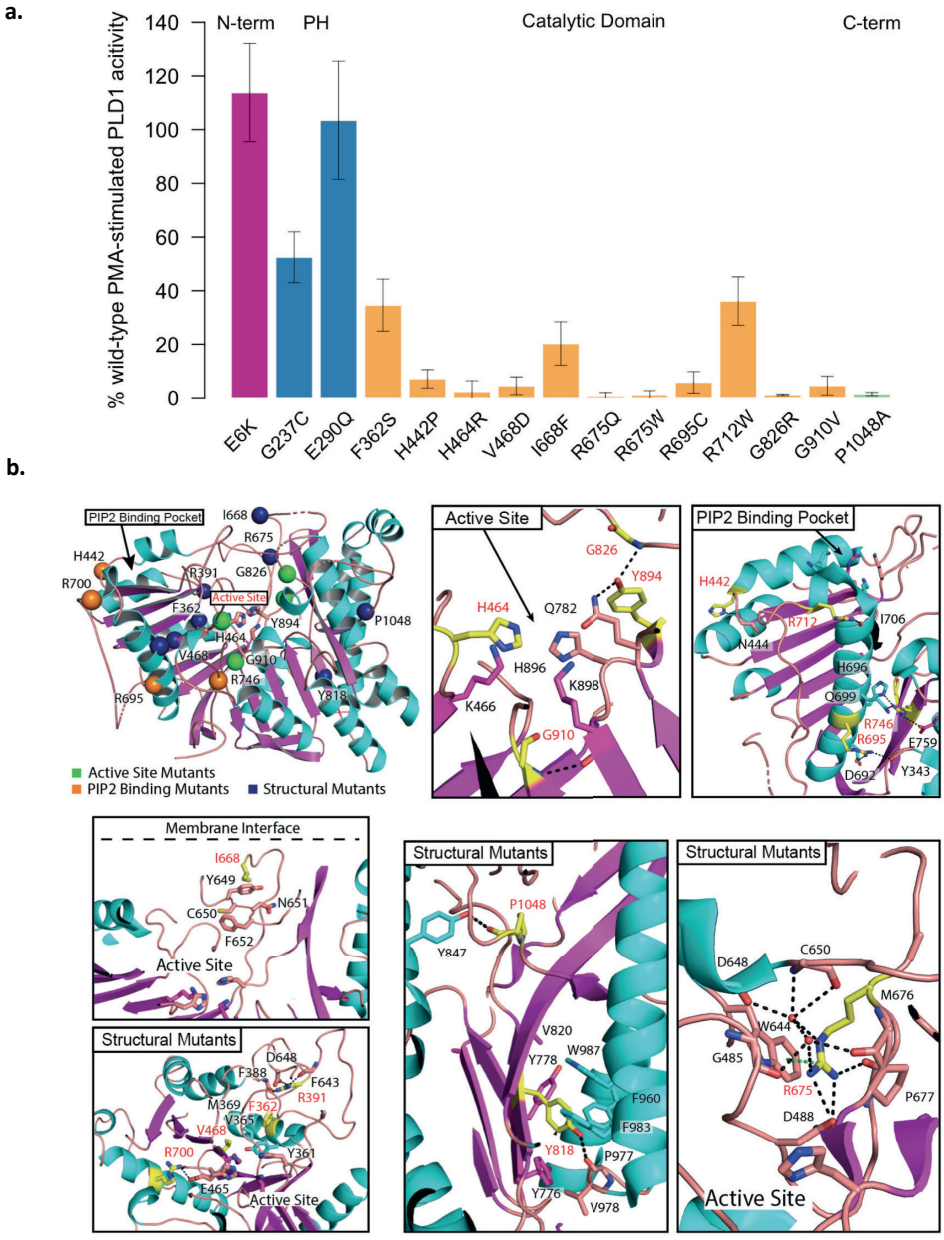


**Figure 2. Activity of pathogenic PLD1 variants and their placement on the 3-D protein structure**. (a) Activity of missense PLD1 variants above the K898R negative control as normalized to the wild-type PLD1 positive control. (b) Placement of missense variants on PLD1 catalytic domain crystal structure. a-Helicies, cyan; b-sheets, magenta. Spheres, pathogenic missense variants. Green spheres, active site variants; orange spheres, PIP2 binding mutants; blue spheres, structural mutants. Insets, closeups of WT residue interactions potentially disrupted by pathogenic variants. Pathogenic residue, yellow stick representation; black dashed line, hydrogen bond; green dashed line, cation-pi interaction. See **Supplemental Videos 2-18** for rotatable presentations and depiction of impact of variants on local structure.

allele in *trans* remains unclear. In contrast, a 50% reduction of activity was observed with p.G237C. We predict this variant may affect membrane binding, as this is the main function of the PH domain[26], and p.G237 is nearby two residues, C240 and C241, which are post-translationally modified by palmitoylation to anchor PLD1 to membranes and are functionally required for PLD1's role in regulating exocytosis.[26–28] We also assessed the location of the eighteen variants found homozygously in the general population of individuals from gnomAD[23], only seven of which localized to the catalytic domain (**Supplemental Figure 5, Supplemental Table 3).** In contrast to the disease-associated missense variants above that are embedded at sites critical for catalysis, these residues all lie on the periphery of the protein with their side-chains facing outwards and making few, if any interactions with other residues. This underscores the importance of evaluating amino acid substitutions in the setting of the 3-dimensional structure. In addition, the disease-associated missense variants were more often predicted to be deleterious and affected residues that were more conserved across species (**Supplemental Fig 6**). Taken together, the disease-associated variants reported here primarily locate to sites critical for catalysis and correspondingly exhibit major loss of enzymatic activity.

## PLD1 is required for endocardial cell EMT in AV cushion explants

Structural atrioventricular valve defects are the cardinal malformation in PLD1 loss-of-function patients. In the embryonic heart, a pivotal early step in valvulogenesis occurs when a subpopulation of endocardial cells overlaying the pro-valvular cardiac cushions undergoes epithelial–mesenchymal transition (EMT).[5] These mesenchymal cells seed the cushions leading to remodelling of the extracellular matrix and contribute to development of the valves and cardiac septa.

To date, many important endocardial cell EMT genes have been identified using an *in vitro* collagen gel assay system (**Supplemental Figure 7**) in which chick embryo atrioventricular cushions (AVC) are excised, transfected, and explanted endocardial-side down onto a collagen pad.[14] The explant myocardium compacts and beats while the endocardial cells spread out and form a surface monolayer. Some of the endocardial cells eventually undergo EMT, seeding the collagen gel with mesenchymal cells. The spatial specificity observed *in vivo*, where the AVC but not the ventricular endocardium undergoes EMT, is reproduced in this *in vitro* assay.[14] We used this assay to investigate the involvement of *PLD1* in endocardial EMT by incubating chick embryo AVC explants with 1-butanol, which suppresses the generation of phosphatidic acid by PLD1, and 3-butanol, which does not suppress phosphatidic acid formation, as a control compound. We observed normal levels of invasion in 3-butanol-treated explants compared to vehicle-

incubated controls (data not shown). 1-butanol incubation, however, significantly reduced the number of transformed cells compared to the 3-butanol-treated controls (**Figure 3a**) suggesting that PLD1 function is involved in endocardial cell EMT *in vitro*.

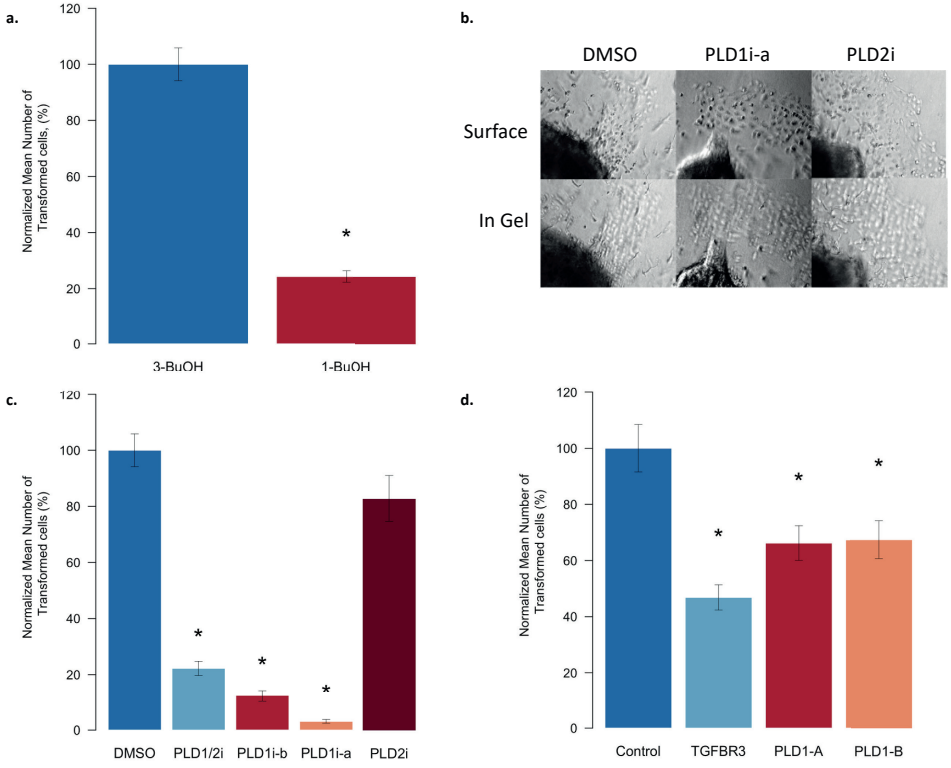


**Figure 3. PLD1 is required for endocardial cell EMT in AV cushion explants *in vitro*.** The role of PLD1 in EMT was determined using a collagen gel assay by incubating Hamburger-Hamilton (HH) stage 16 chick atrioventricular canal (AVC) cushion explants on collagen gels for 48 hours with chemical (**a**), small molecule inhibitors (**b-c**) of PLD or siRNA (**d**). The number of cells undergoing EMT per explant were counted for each condition and normalized over 3 separate experiments to relevant control explants (100%). (**a**) HH16 AVC explants were incubation with either 0.6% normal butanol (1-BuOH, which inhibits PLD generation of PA), or tertiary butanol (3-BuOH), which does not inhibit PA production. n=30 explants for each condition. * - p<0.01 compared to control. (**b**) Representative photomicrographs of AVC explants on collagen gels incubated with 500nM doses of small molecule inhibitors (i) of PLD1i-a (VU0359595), PLD2i (VU0285655-1), or DMSO. (**c**) HH16 AVC explants (n=30 for each condition) were incubated with small molecule PLD inhibitors or DMSO. PLD1/2i (VU0155056) inhibits both PLD1 and PLD2; PLD1i-B (VU0155069) selectively inhibits PLD1. (**d**) HH16 AVC explants were incubated with siRNAs targeting *TGFβR3,* two different regions of *PLD1-A/B*, or scrambled siRNA (control). Control (n=19) explants, GC-content matched, randomized siRNA constructs with no homology to any known chick gene. *TGFβR3* (n=23) - siRNA targeting a gene known to be required for EMT *in vitro*. PLD1-A (n=26) or PLD1-B (n=25) - independent constructs targeting different regions of PLD1. * - p<0.05 compared to control. * - p<0.01 compared to control. All p-values calculated using Student's T-test.

The role of PLD1 was then confirmed using PLD small molecule inhibitors[29]. PLD1 inhibition dramatically reduced the number of transformed cells, whereas no reduction was seen using an inhibitor of PLD2, the other classic member of the PLD superfamily (**Figure 3b-c**). Similarly, siRNA constructs targeting chick PLD1 significantly decreased the number of transformed cells compared to a scrambled control (**Figure 3d**). siRNA targeting TGFβR3, which is required for endocardial cell EMT in AVCs[30], was used as a positive control. Finally, PLD1 inhibition did not decrease endocardial cell proliferation or increase cell death (**Supplemental Figure 8c-d, Supplementary Note 2).** Together, these data indicate that PLD1 is required for endocardial cell EMT, a pivotal early step in valvulogenesis, and suggest that abnormal EMT may underlie, at least in part, the cardiac structural malformations in patients with loss-of-function bi-allelic *PLD1* variants.

Downstream mechanisms whereby loss of PLD1 enzymatic activity leads to right sided atrio-ventricular valve defects could entail established crosstalk between PLD1 signalling and TGF-beta signalling.[31] In the heart, TGF-beta signalling is crucial for the formation of the mesenchyme of the cardiac cushions and the EMT necessary for cardiac valve formation.[32,33] For example, transgenic TGFB2 mice have abnormal atrioventricular valve morphology and pulmonary artery hypoplasia amongst other phenotypes.[34] It may also involve sonic hedgehog (Shh) expression, which can be stimulated by TGF-beta signalling.[35,36] Shh becomes expressed in the pharyngeal endoderm adjacent to the secondary heart field, where it maintains secondary heart field cell proliferation, which is required for normal arterial pole formation.[37] Interestingly, even moderate inhibition of sonic hedgehog signaling at this developmental stage leads to pulmonary atresia as the main phenotype. Thus, possible pathophysiological mechanism for loss-of-function PLD1 variants to be investigated in future studies might involve a reduction in TGF-beta and sonic hedgehog signaling, which could result in arterial pole defects as seen in the patients.

In conclusion, we identified 29 patients from 20 families with a spectrum of severe cardiac disorders caused by loss-of-function bi-allelic variants in *PLD1*. We show that p.I668F is a recessive founder variant among the Ashkenazi Jews. While further studies are required, genotyping of the p.I668F founder variant, which has a MAF of 2% among the Ashkenazi Jews, could potentially be utilized in population-based preconception and prenatal carrier screening to asses risk of congenital heart defects among descendants of Ashkenazi Jews.[38] We demonstrated that missense variants in PLD1 cluster in regions of the protein known to be critical for catalytic activity and predominantly result in a strong enzymatic loss-of-function. Using an *in vitro* system we show that PLD1 is implicated in EMT, an established pivotal early step in valvulogenesis, providing a possible mechanism whereby loss of PLD1 function may lead to the observed cardiac defects. We expand the

phenotypic spectrum of *PLD1*-associated congenital heart defects and provide evidence that recessive variants in *PLD1* can also cause neonatal cardiomyopathy in the absence of congenital heart defects, a manifestation not previously associated with this gene. Together, these data provide an increased understanding of disease mechanisms and phenotypic expression associated with genetic defects in *PLD1*.

# REFERENCES


1 Dolk H, Loane M, Garne E, European Surveillance of Congenital Anomalies (EUROCAT) Working Group. Congenital Heart Defects in Europe: Prevalence and Perinatal Mortality, 2000 to 2005. *Circulation* 2011; 123: 841–849.

2 Ta-Shma A, Zhang K, Salimova E *et al.* Congenital valvular defects associated with deleterious mutations in the PLD1 gene. *J Med Genet* 2017; 54: 278–286.

3 Sobreira N, Schiettecatte F, Valle D, Hamosh A. GeneMatcher: A Matching Tool for Connecting Investigators with an Interest in the Same Gene. *Hum Mutat* 2015; 36: 928–930.

4 Bowling FZ, Salazar CM, Bell JA, Huq TS, Frohman MA, Airola M V. Crystal structure of human PLD1 provides insight into activation by PI(4,5)P2 and RhoA. *Nat Chem Biol* 2020; 16: 400–407.

5 Barnett J V., Desgrosellier JS. Early events in valvulogenesis: A signaling perspective. *Birth Defects Res Part C Embryo Today Rev* 2003; 69: 58–72.

6 Velde ET Vander, Vriend JWJ, Mannens MMAM, Uiterwaal CSPM, Brand R, Mulder BJM. CONCOR, an Initiative towards a National Registry and DNA-Bank of Patients with Congenital Heart Disease in the Netherlands: Rationale, Design, and First Results. Eur. J. Epidemiol. 2005; 20: 549–557.

7 Gelb B, Brueckner M, Chung W *et al.* The Congenital Heart Disease Genetic Network Study. *Circ Res* 2013; 112: 698–706.

8 Jin SC, Homsy J, Zaidi S *et al.* Contribution of rare inherited and de novo variants in 2,871 congenital heart disease probands. *Nat Genet* 2017; 49: 1593–1601.

9 Morris AJ, Frohman MA, Engebrecht J. Measurement of Phospholipase D Activity. *Anal Biochem* 1997; 252: 1–9.

10 Altshuller YM, Altshuller YM, Sung TC *et al.* Human ADP-ribosylation Factor-activated Phosphatidylcholine-specific Phospholipase D Defines a New and Highly Conserved Gene Family. *J Biol Chem* 1995; 270: 29640–29643.

11 Leiros I, Secundo F, Zambonelli C, Servi S, Hough E. The first crystal structure of a phospholipase D. *Structure* 2000; 8: 655–67.

12 Dixon JE, Stuckey JA. Crystal structure of a phospholipase D family member. *Nat Struct Biol* 1999; 6: 278–284.

13 Sung T-C. Mutagenesis of phospholipase D defines a superfamily including a trans-Golgi viral protein required for poxvirus pathogenicity. *EMBO J* 1997; 16: 4519–4530.

14 DeLaughter DM, Saint-Jean L, Baldwin HS, Barnett J V. What chick and mouse models have taught us about the role of the endocardium in congenital heart disease. *Birth Defects Res Part A Clin Mol Teratol* 2011; 91: 511–525.

15 Townsend TA, Robinson JY, How T, DeLaughter DM, Blobe GC, Barnett J V. Endocardial cell epithelial-mesenchymal transformation requires Type III TGFβ receptor interaction with GIPC. *Cell Signal* 2012; 24: 247–56.

16 Townsend TA, Wrana JL, Davis GE, Barnett J V. Transforming growth factor-beta-stimulated endocardial cell transformation is dependent on Par6c regulation of RhoA. *J Biol Chem* 2008; 283: 13834–41.

17 Townsend TA, Robinson JY, Deig CR *et al.* BMP-2 and TGFβ2 shared pathways regulate endocardial cell transformation. *Cells Tissues Organs* 2011; 194: 1–12.

18 Chang CC, Chow CC, Tellier LC, Vattikuti S, Purcell SM, Lee JJ. Second-generation PLINK: rising to the challenge of larger and richer datasets. *Gigascience* 2015; 4: 7.

19 Belkadi A, Pedergnana V, Cobat A *et al.* Whole-exome sequencing to analyze population structure, parental inbreeding, and familial linkage. *Proc Natl Acad Sci* 2016; 113: 6713–6718.
20 Bray SM, Mulle JG, Dodd AF, Pulver AE, Wooding S, Warren ST. Signatures of founder effects, admixture, and selection in the Ashkenazi Jewish population. *Proc Natl Acad Sci U S A* 2010; 107: 16222–7.
21 Gandolfo LC, Bahlo M, Speed TP. Dating Rare Mutations from Small Samples with Dense Marker Data. *Genetics* 2014; 197: 1315–1327.
22 van der Palen RLF, van der Wal AC, Robles de Medina PG, Blom NA, Clur S-AB. Uhl's anomaly: Clinical spectrum and pathophysiology. *Int J Cardiol* 2016; 209: 118–21.
23 Karczewski KJ, Francioli LC, Tiao G *et al.* The mutational constraint spectrum quantified from variation in 141,456 humans. *Nature* 2020; 581: 434–443.
24 Sung T-C, Zhang Y, Morris AJ, Frohman MA. Structural Analysis of Human Phospholipase D1. *J Biol Chem* 1999; 274: 3659–3666.
25 Hammond SM, Altshuller YM, Sung TC *et al.* Human ADP-ribosylation factor-activated phosphatidylcholine-specific phospholipase D defines a new and highly conserved gene family. *J Biol Chem* 1995; 270: 29640–3.
26 Du G, Altshuller YM, Vitale N *et al.* Regulation of phospholipase D1 subcellular cycling through coordination of multiple membrane association motifs. *J Cell Biol* 2003; 162: 305–15.
27 JM S, S C, M M, J C, NT K. Fatty Acylation of Phospholipase D1 on Cysteine Residues 240 and 241 Determines Localization on Intracellular Membranes. *J Biol Chem* 1999; 274. doi:10.1074/JBC.274.42.30023.
28 Vitale N, Caumont A, Chasserot-Golaz S *et al.* Phospholipase D1: a key factor for the exocytotic machinery in neuroendocrine cells. *EMBO J* 2001; 20: 2424–2434.
29 Lavieri RR, Scott SA, Selvy PE *et al.* Design, synthesis, and biological evaluation of halogenated N-(2-(4-oxo-1-phenyl-1,3,8-triazaspiro[4.5]decan-8-yl)ethyl)benzamides: discovery of an isoform-selective small molecule phospholipase D2 inhibitor. *J Med Chem* 2010; 53: 6706–19.
30 Bassing CH, Yingling JM, Howe DJ *et al.* A transforming growth factor beta type I receptor that signals to activate gene expression. *Science* 1994; 263: 87–9.
31 Piazza GA, Ritter JL, Baracka CA. Lysophosphatidic Acid Induction of Transforming Growth Factors α and β: Modulation of Proliferation and Differentiation in Cultured Human Keratinocytes and Mouse Skin. *Exp Cell Res* 1995; 216: 51–64.
32 Xu J, Lamouille S, Derynck R. TGF-β-induced epithelial to mesenchymal transition. *Cell Res* 2009; 19: 156–172.
33 Gise A von, Pu WT. Endocardial and epicardial epithelial to mesenchymal transitions in heart development and disease. *Circ Res* 2012; 110: 1628.
34 Sanford LP, Ormsby I, Groot ACG *et al.* TGFβ2 knockout mice have multiple developmental defects that are non-overlapping with other TGFβ knockout phenotypes. *Development* 1997; 124: 2659.
35 Javelaud D, Alexaki VI, Dennler S, Mohammad KS, Guise TA, Mauviel A. TGF-β/SMAD/GLI2 signaling axis in cancer progression and metastasis. *Cancer Res* 2011; 71: 5606–10.
36 Dennler S, André J, Alexaki I *et al.* Induction of Sonic Hedgehog Mediators by Transforming Growth Factor-β: Smad3-Dependent Activation of *Gli2* and *Gli1* Expression *In vitro* and *In vivo*. *Cancer Res* 2007; 67: 6981–6986.
37 Dyer LA, Kirby ML. Sonic hedgehog maintains proliferation in secondary heart field progenitors and is required for normal arterial pole formation. *Dev Biol* 2009; 330: 305–317.
38 Slatkin M. A population-genetic test of founder effects and implications for Ashkenazi Jewish diseases. *Am J Hum Genet* 2004; 75: 282–93.